J Nanostruct 16(4): 4976-4986, Autumn 2026

RESEARCH PAPER

Eco-Friendly Synthesis of Iron Disulfide (FeS_2) Nanoparticles Using Artemisia Herba-Alba Extract and Evaluation of Their Antibacterial Activity

Ahmed Aziz Ali *, Hameed Khalid Al

Department of Chemistry, College of Education for Pure Sciences, University of Anbar, Ramadi, Anbar, Iraq

ARTICLE INFO

Article History:
Received 27 May 2026
Accepted 17 August 2026
Published 01 October 2026

Keywords:
Antibacterial activity
Artemisia herbal-alba
FeS_2 nanoparticles
Green synthesis

ABSTRACT

This work Explored the biogenic synthesis of Iron disulfide nanoparticles (FeS_2 NPs) using a water extract of Artemisia herbal-alba (wormwood) plant as a reducing and capping agent, instead of the conventional physicochemical synthesis that uses toxic chemicals and severe conditions. An aqueous extract of wormwood was prepared by extracting dried powder of the leaves at 70-80°C, and was mixed with ferrous sulfate and sodium sulfide (0.02 M) solutions to form an iron sulfide (FeS) precipitate, which was then sulfurized thermally at 300°C to produce pure pyrite. Rigorous physicochemical characterization provided accurate results; FTIR analysis confirmed the presence of active phytochemicals (phenolic, flavonoids and terpenoids) on the surface of nanoparticles, and X-ray diffraction (XRD) confirmed the pure crystalline phase with an average crystallite size of about 10 nm, calculated using the Debye-Scherrer equation. TEM analysis showed quasi-spherical to irregular shapes and sizes of 25-70 nm, and EDX confirmed high purity. Pragmatically, the nanoparticles showed concentration-dependent antibacterial action against Staphylococcus aureus and Escherichia coli, with an inhibition zone of 17 mm and 15 mm, respectively, at the highest concentration. This is explained by several mechanisms, such as membrane damage, induction of oxidative stress through Fenton reactions, and sulfur radicals. Taken together these results demonstrate the feasibility of green nanotechnology for sustainable biomedical applications antimicrobial agents for prospective biomedical and environmental applications

How to cite this article
Aziz Ali A., Khalid Al H. Eco-Friendly Synthesis of Iron Disulfide (FeS_2) Nanoparticles Using Artemisia herba-alba Extract and Evaluation of Their Antibacterial Activity. J Nanostruct, 2026; 16(4):4976-4986. DOI: 10.22052/JNS.2026.04.042

INTRODUCTION

Nanotechnology is gaining significant interest among scientists due to the unique properties of materials at the nanometer scale (1 billionth of a meter). Nanomaterials possess a greater surface area and distinctive physical and chemical properties compared to larger materials, making them suitable for various applications in medicine, the environment, and energy [1]. Materials such as Iron Disulfide (FeS_2) are considered by the environmental sciences to be a viable alternative for biological and environmental applications. Iron Disulfide has demonstrated exceptional chemical stability with excellent electrical and

* *Corresponding Author Email: ahm24u4005@uoanbar.edu.iq*

magnetic properties [2]. Conventional techniques for the production of nanoparticles are primarily physical or chemical methods that involve the use of toxic, hazardous materials and/or require high temperature and pressure conditions. As a result, the use of these methods and subsequently produced materials are not suitable for the biological field due to potential negative effects on the environment and on consumer health [3]. Therefore, it is necessary to develop viable green alternatives to conventional nanoparticle preparation methods; specifically, green preparation methods that utilize the reducing and stabilizing properties of biological material (plant extracts and microorganisms) [4].Additionally, many secondary plant metabolites (e.g., phenolics, flavonoids, terpenoids and alkaloids) are responsible for stabilizing chloroplasts and serve to reduce metal ions to form nanoparticles that are more stable and have a higher degree of biocompatibility than those fabricated using standard methods [5]. Studies demonstrating the efficacy of producing both metallic and sulfide nanoparticles having measurable biologic activity have been published [6]. Plants of the Artemisia genus are known for their medicinal properties and contain many bioactive compounds that exhibit activity against bacteria, fungi, and free radicals. Artemisia extracts have been shown to be effective agents for producing stable nanoparticles with higher levels of biological activity as a result of coating nanoparticles with active compounds from the Artemisia plant. [7,8] While many studies have reported use of green synthesis for metallic nanoparticles, very few have examined green synthesis of iron disulfide (FeS_2) nanoparticles from plant extracts. Therefore, there is much potential for further work in this area. Assessment of the biological activity of these nanoparticles is required to understand how they work and what their potential uses may be in both medicine and the environment [9].The goal of this study is to produce nanoparticles of iron disulfide by green synthesis using extracts from Artemisia absinthian, and to evaluate the biological activity of those nanoparticles, as such will enable development of sustainable and environmentally responsible nanotechnology [10].

MATERIALS AND METHODS

Artemisia herba-alba leaf extract preparation

Leaves of Artemisia herba-alba were harvested in their natural habitat and washed thoroughly with sterile distilled water to remove any

Fig. 1. Steps for preparing Artemisia herbal-alba leaf extract.

impurities or debris. The harvested leaves were then laid flat in a shady place, without any direct sunlight, for one week until they were completely dried [11]. After the drying process, the harvested leaves were thoroughly ground into a fine powder and used for extraction by weighing out one gram of Artemisia herba-alba powder into a glass flask containing 100 ml of sterile distilled water. The flask with the powder and water was placed on an electric hot plate, with a temperature between 70ºC and 80ºC, and a magnetic stirrer at 1.5 hours [12,13]. After the heating process, the solution was cooled to room temperature and filtered to yield the extract. The extract was then placed in a bottle for storage in the refrigerator and for use in the creation of iron-sulfur nanoparticles, as shown in Fig. 1.

Preparation of iron disulfide NPs

An iron sulfide (FeS) solution at a molarity of 0.02M has been created by dissolving 0.312 g sodium sulfide (Na_2S) in 200 ml of distilled water and 0.612 g iron sulfate ($FeSO_4$) in 200 ml of distilled water [14]. To prepare the mixture, 200 ml of the iron sulfate solution was prepared with 200 ml wormwood leaf extract using a magnetic stirrer for 30 minutes. The sodium sulfide was added to the glass flask with the iron sulfate solution and wormwood leaf extract by burr distilling into droplets into the flask while stirring continuously to achieve equal distribution of the droplets throughout the solution [15]. The resulting mixture will stand for 24 hours to allow precipitation to occur. The precipitate formed in the resulting mixture is separated by centrifuging. After centrifuging, the precipitate is dried in an oven at 80 degrees Centigrade for 24 hours. The resulting product is FeS [16]. To convert this to iron disulfide nanoparticles, pure sulfur is added in a 1:1 ratio to the precipitate, placed in a container, and then set on fire (burning) at a temperature of 300 degrees Centigrade for 3 hours. The resulting product is then washed in distilled water and ethanol, dried completely, and ground into very fine particles, producing iron disulfide nanoparticles) FeS_2), as shown in Fig. 2.

Evaluation of the Antibacterial Activity of FeS_2 Nanoparticles

The antibacterial activity of the prepared iron disulfide nanoparticles (FeS_2 NPs) was evaluated against two commonly encountered clinical pathogens: Staphylococcus aureus (Gram-positive) and Escherichia coli (Gram-negative) bacteria, with different types of bacterial cell wall surface structures. The bacterial strains were cultured on nutrient agar plates and incubated under standard culture conditions (37 °C for 24 hours). A bacterial suspension was then prepared and adjusted to the turbidity of the 0.5 McFarland standards

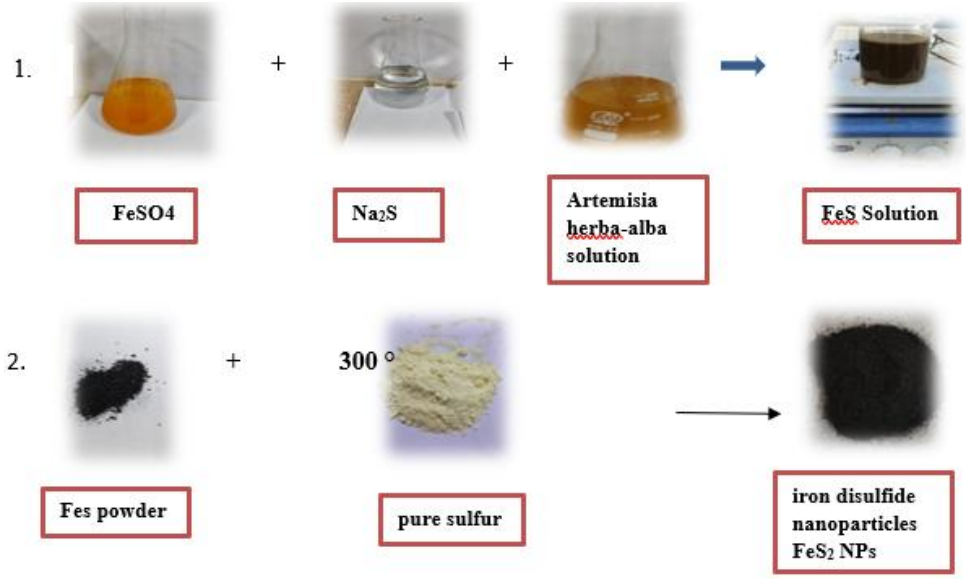

Fig. 2. Preparation steps of iron disulfide (FeS_2) nanoparticles.

(approximately 1.5 x 10^8 CFU/Ml) [17-18]. The agar well diffusion method was used to determine the antibacterial activity, a standard technique for initial screening of antibacterial drugs. After the inoculated agar surface had solidified, four equidistant wells were aseptically bored into the agar in each plate using a sterile corn borer of a fixed diameter. The wells were filled in the following manner: Wells A, B, and C: Dilutions of FeS_2 nanoparticle suspensions, prepared at 100%, 50% and 25% (v/v), respectively. Well D (Negative Control): Sterile distilled water (no nanoparticles) to ensure that no inherent solvent-mediated antibacterial activity was present. The plates were then incubated at 37 °C for 24 hours. After the incubation period, the antibacterial efficacy was assessed by measuring the zone of inhibition (in millimeters) around the wells using a ruler. The absence of inhibition around the control well (D) confirmed that the observed bacteriostatic or bactericidal activity was only due to the FeS_2 nanoparticles. The minimum inhibitory concentration (MIC) was subsequently determined as the lowest concentration of nanoparticles displaying a visible zone of inhibition, which is indicative of substantial inhibition of bacterial growth. Similarly, the minimum bactericidal concentration (MBC) was defined as the lowest concentration of nanoparticles that completely eliminated visual bacterial growth, indicative of permanent bactericidal effect [19].

RESULTS AND DISCUSSION

FT-IR Test

It is to find out the active compounds in chemical compounds [20] FTIR spectrum of Artemisia powder has different functional groups of bioactive phytoconstituents. The peak in the region 3200-3500 cm-1 is due to the stretching vibration of O-H, which may be due to hydrogen bonding of phenolic and alcoholic compounds. The asymmetric and symmetric stretching vibration of aliphatic C-H (2920 and 2850 cm^{-1}) is due to the presence of the hydrocarbon/torpedoed. The peaks of 1600-1650 cm-1 are related to the stretching vibration of C=O. They may also be due to C=C (aromatic ring), and prove the presence of carbonyl and aromatic groups. The other peaks at range 1000-1300 cm^{-1} are due to alcohol C-O stretching vibration mode, and also due to C-O stretching vibration mode of glycoside linkage, respectively. This shows the presence of hydroxyl, carbonyl, aromatic and aliphatic groups, which also suggest the phytochemical variability of Artemisia as a good natural reducing and stabilizing agent for the green synthesis of nanoparticles, as shown in Fig. 3.

FT-IR spectroscopy of iron disulfide

There was a broad band present from 3367

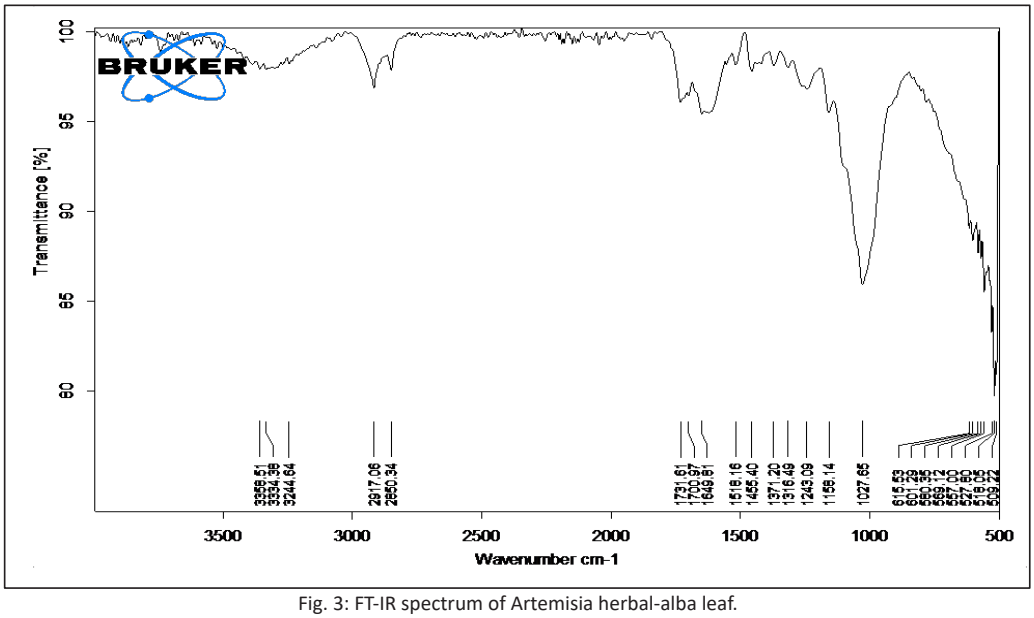

Fig. 3: FT-IR spectrum of Artemisia herbal-alba leaf.

to 3197 cm^{-1}; this was caused by O-H and N-H stretching vibrations of phenolic compounds and proteins that are present in the extract of the plant. Other bands, which appeared from 2924 to 2853 cm^{-1}, corresponded to aliphatic C-H stretching, and from 1450 to 1380 cm^{-1}, corresponded to aromatic C=C vibrations. The bands between 620 and 520 cm^{-1} are related to Fe-S (iron-sulfur) vibrations, which indicate that the nanoparticles were successfully created. These functional groups suggest that the plant constituents serve as both reducing and stabilizing agents for the nanoparticles [21, 22] as shown in Fig. 4.

Transmission Electron Microscopy (TEM)

The morphological properties and particle size distribution of the green-synthesized iron disulfide (FeS_2) nanoparticles from Artemisia plant extract were examined using Transmission Electron Microscopy (TEM). The TEM micrographs show the formation of nanoscale particles with predominantly quasi-spherical and irregular

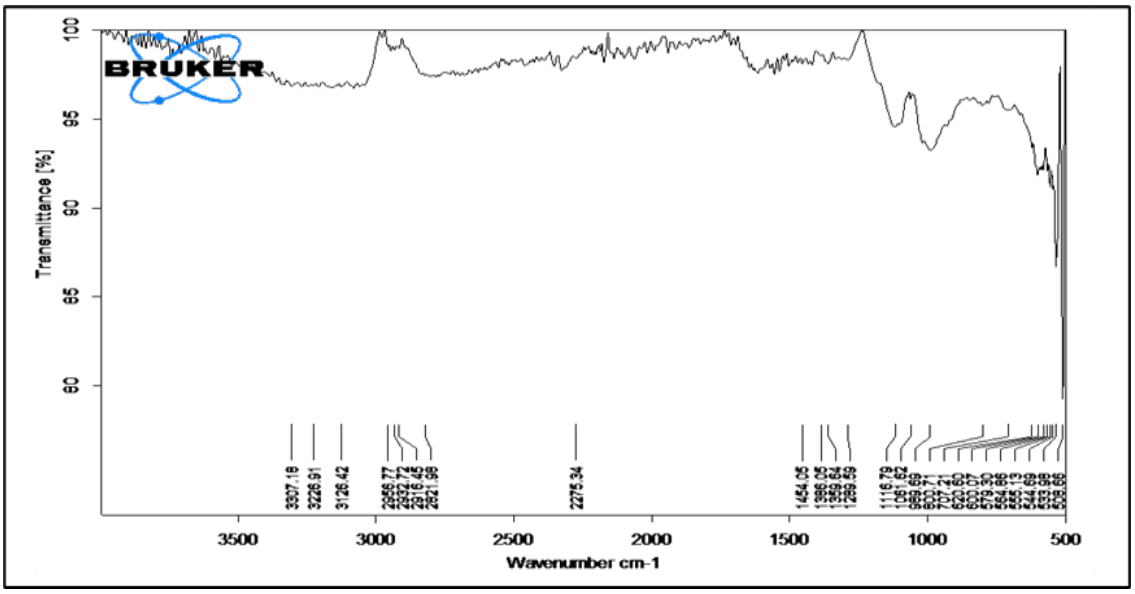

Fig. 4. Spectrum of iron disulfide.

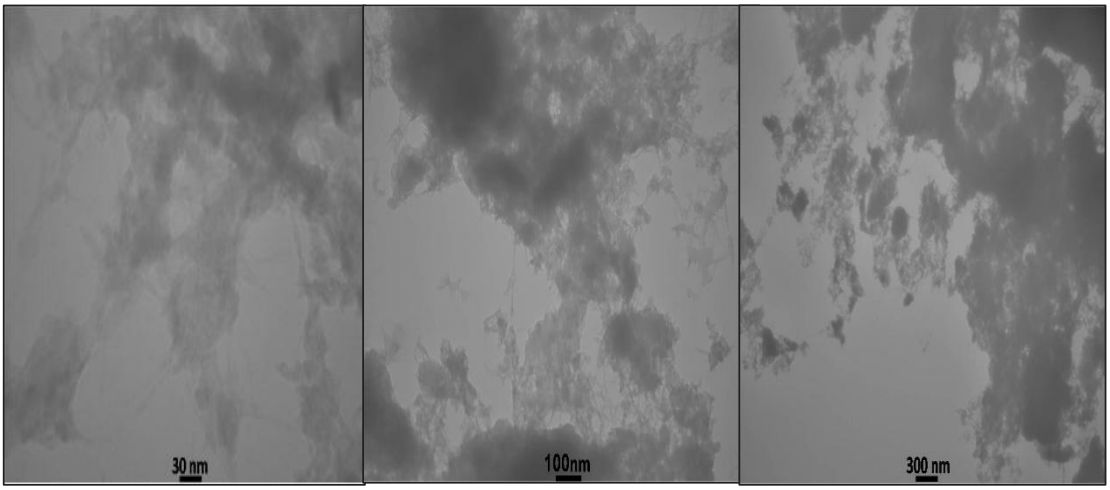

Fig. 5. TEM micrographs of iron disulfide NPs.

shapes. A noticeable degree of agglomeration was The Transmission Electron Microscopy (TEM) analysis has characterized the morphological properties and particle size distribution of green-synthesized iron disulphide (FeS_2) nanoparticles derived from Artemisia plant extract. The images show the synthesis of nanoparticles, mostly quasi-spherical to irregularly shaped particles, with considerable aggregation resulting in the formation of interconnected cluster-like aggregates. This agglomeration is attributed to the large surface area of the nanoparticles compared to their volume, leading to higher surface energy and mutual attraction between nanoparticles. At higher magnifications (scale bars 100 nm and 30 nm), individual nanoparticles can be seen ranging from 25 nm to 70 nm in diameter. The size distribution is rather broad (polydisperse), which is typical for nanoparticles biosynthetically derived due to differences in nucleation and crystal growth. The TEM micrographs show significant contrast differences, with darker areas corresponding to FeS_2 nanoparticles (from their electron density) against a background of lighter regions that represent either the supporting carbon film or thinner parts of the sample. In summary, the TEM images confirm the synthesis of binaural-sized FeS_2 nanoparticles with typical

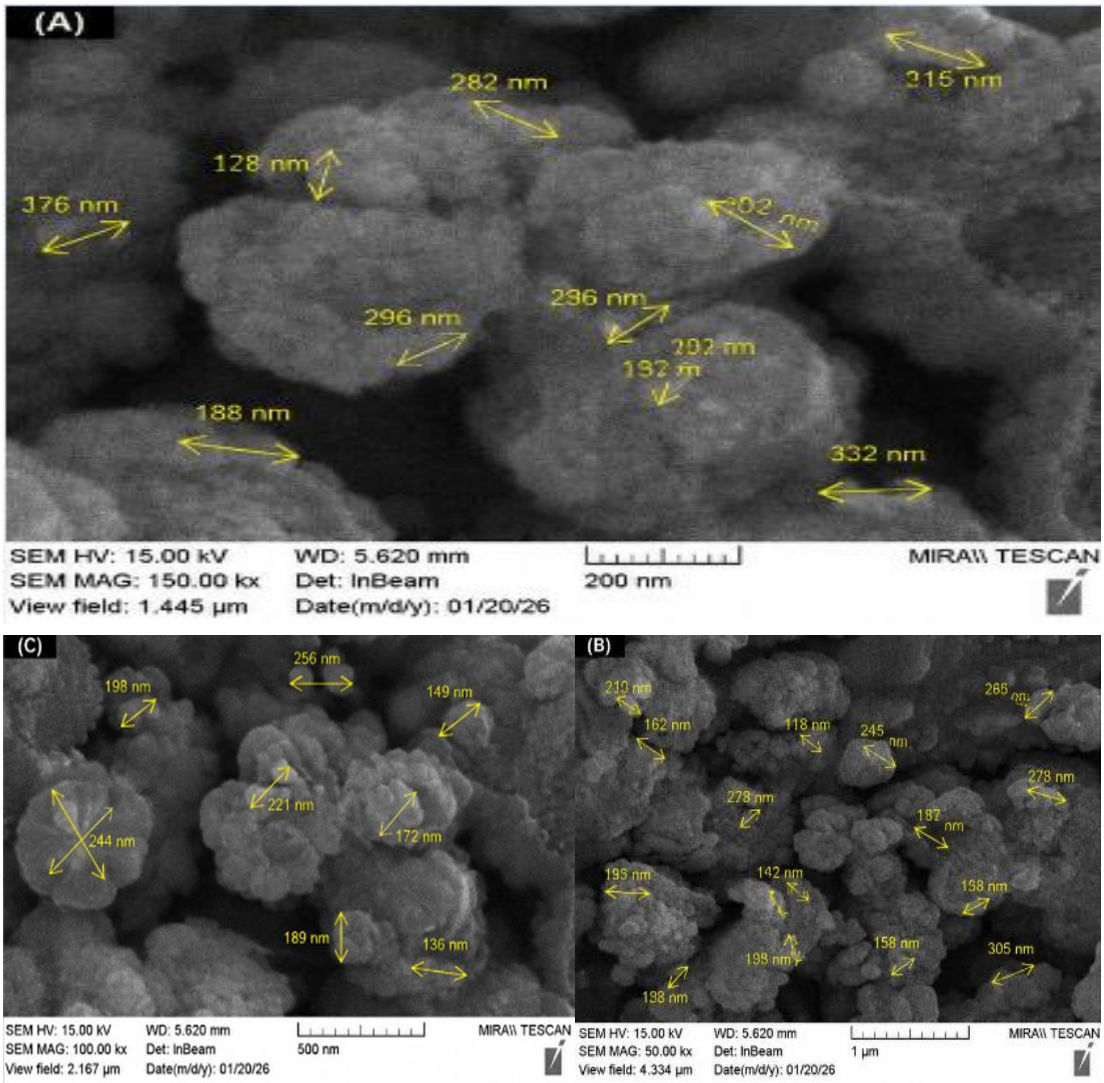

Fig. 6. SEM images of iron disulfide NPs.

morphological features of biologically produced nanoparticles [23] as in Fig. 5.

Scanning electron microscopy (SEM)

The shape and size of the green-synthesized iron disulphide (FeS_2) nanoparticles from the Artemisia plant extract were determined by Transmission Electron Microscopy (TEM). The TEM images reveal the synthesis of nanoscale particles with mostly quasi-spherical and irregular shaped particles. A noticeable degree of agglomeration was The Transmission Electron Microscopy (TEM) analysis has characterized the morphological properties and particle size distribution of green-synthesized iron disulphide (FeS_2) nanoparticles derived from Artemisia plant extract. In the images, the formation of nanoparticles, predominantly quasi-spherical and irregular particles, with significant degree of agglomeration leading to cluster-like aggregates is presented. The agglomeration is due to the high surface-to-volume ratio of the nanoparticles which results in enhanced surface energy and attraction between nanoparticles. At higher magnifications (scale bars 100 nm and 30 nm), individual nanoparticles with sizes between 25 nm and 70 nm in diameter can be observed. The size distribution is relatively wide (polydisperse) as is common for biosynthetically produced nanoparticles due to variations in nucleation and growth of the crystals. In the TEM images, there exists a strong contrast between dark regions of FeS_2 nanoparticles (from their electron density) and the lighter regions which may be the carbon film supporting the sample, or thinner regions of

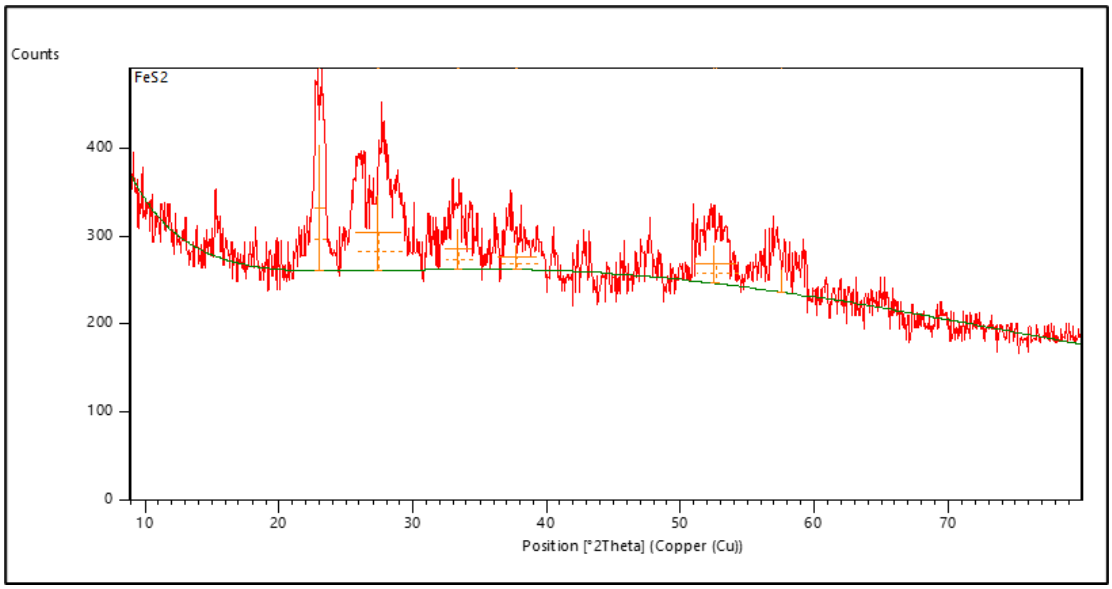

Fig. 7. XRD pattern of Iron disulfide NPs.

Table 1. XRD pattern of Iron disulfide NPs.

Position (2θ deg.)	FWHM (deg.)	Intensity (count)
22.98	0.84	145
27.34	3.50	88
33.32	2.00	46
52.54	3.10	44

the sample. Overall, the TEM images show the formation of binaural-sized FeS_2 nanoparticles with common morphological characteristics of biological nanoparticles [24] as in Fig. 6.

XRD Characterization

Fig. 7 shows the-ray diffraction (XRD) patterns of iron disulfide (FeS_2) nanoparticles prepared using the green synthesis method showed distinct crystalline peaks at 2θ values of approximately 22.98°, 27.34°, 33.32°, 37.70°, 52.54°, and 57.53°, indicating the formation of a crystalline pyrite phase consistent with standard ICDD/JCPDS data. The absence of additional peaks indicates the purity of the formed phase and the lack of significant secondary phases. Broadening was also observed in some of the diffraction peaks, a characteristic behavior of nanomaterials and attributable to the small crystal size. The average crystal size was estimated using the Debye–Scherrer equation to be approximately 10 nm, further confirming the nanoscale nature of the material [25].

Energy-dispersive X-ray spectroscopy (EDX)

The surface and shape of the nanoscale materials produced by this green process, as well as elemental composition from EDX, confirm that these materials are of high purity. EDX also indicated that there are no significant trace amounts of metallic elements, suggesting high purity of material in addition to having the characteristic spectrum and composition of

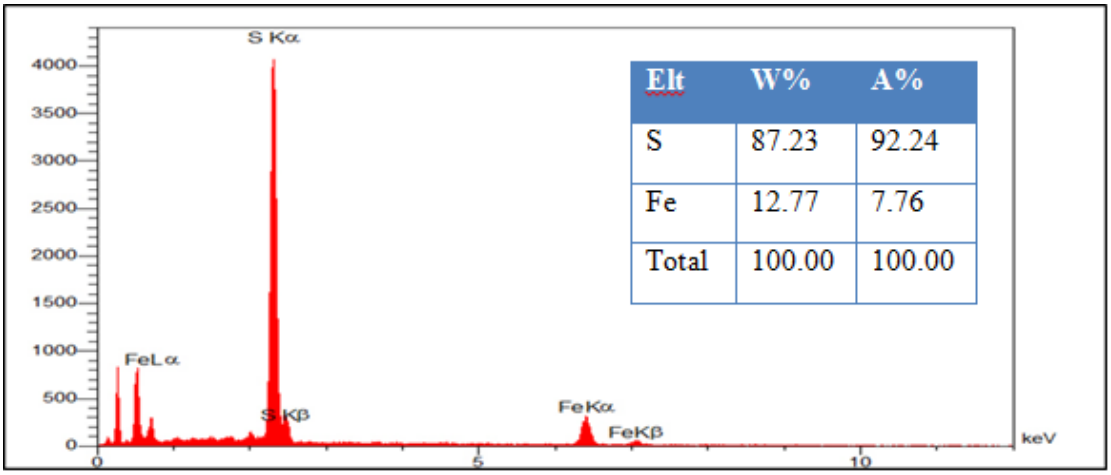

Fig. 8. Energy dispersive X-ray spectroscopy of the prepared iron disulfide NPs.

Table 2. Bacterial growth response to (FeS_2 NPs) at different concentrations.

Hole	Concentration (%)	Staphylococcus aureus(mm)	Escherichia coli (mm)	Interpretation
A	25%	6 mm	5 mm	Weak inhibition (MIC approx)
B	100%	17 mm	15 mm	Strong bactericidal activity
C	50%	11 mm	10 mm	Moderate inhibition
D	Control (0%)	0 mm	0 mm	No inhibition

FeS_2. So, we can conclude that we successfully synthesized high-purity FeS_2 nanoparticles using green synthesize method [26]. as shown in the following Fig. 8.

Evaluation of the antibacterial efficacy of iron disulfide nanoparticles (FeS_2)

In this study, iron disulfide nanoparticles (FeS_2 NPs) biosynthesized were assessed for their anti-bacterial activity against Staphylococcus aureus (Gram-positive) and Escherichia coli (Gram-negative). The activity was evaluated by agar well diffusion method, using four wells i.e. well A, well B, well C and well D representing 25%, 100%, 50% and a negative control (sterile distilled water) respectively. This was performed in order to isolate the different effects that may be introduced by changing the concentration. The experimental protocols and conditions followed were per [27]. The study suggests the induction of a concentration-dependent antibacterial response upon treatment with the FeS_2 NPs. A higher concentration of undiluted FeS_2 NPs equivalent to 100% showed significantly larger zones of inhibition against the two strains of bacteria tested in the study, showing a very potent bactericidal activity in the maximum concentration. An effective bacteriostatic activity could also be recorded upon

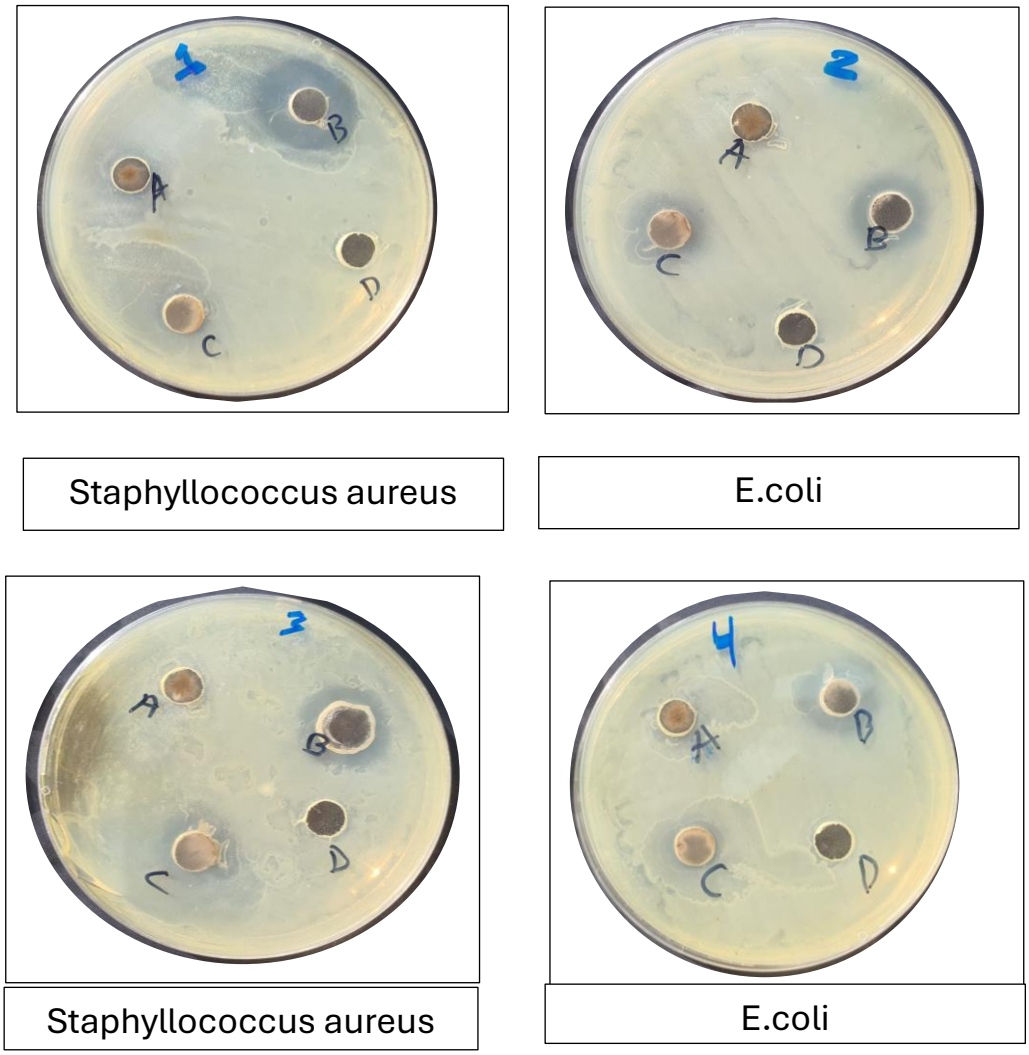

Fig. 9. Antibacterial effect of iron disulfide nanoparticles against *S.aureus* and *E. coli* at different concentrations compared to control.

using an intermediate concentration of 50% from well C, proving that a sub-maximal dose is capable of suppressing the growth of bacterial strains to some extent. The least effective concentration used being 25% from well A showed only a faint zone of inhibition showing partial but not negligible antimicrobial potency. The concentrations were indicative of a minimum inhibitory concentration (MIC) value or threshold required for the exertion of antibacterial properties against the two strains of bacteria under test. A negative control used from well D showed no visible zone of inhibition. This was representative of the fact that only the FeS_2 nanoparticles and not the solvent used have shown antibacterial activity. It is proposed that the superior antibacterial effect of FeS_2 NPs can be mechanistically explained by their nanoscale nature and highly increased surface-area-to-volume ratio, which can lead to stronger interactions with the outer bacterial cell membranes. This interaction would be understood to result in breaking down of the structural integrity of the membrane bilayer, enhancement of membrane permeability, and release of intracellular bacterial constituents. The FeS_2 NPs is thought to be cytotoxic due to the generation of oxidative stress, 2~ mediated through oxidation by iron-catalyzed Fenton-type reactions combined with simultaneous formation of reactive sulfur species (RSS) [28,29]. These reactive species cause oxidative damage to vital biomolecules (structural proteins, membrane lipids and genomic DNA) leading to the loss of bacterial cellular homeostasis and death. Overall, the findings demonstrate the potent broad spectrum antibacterial activity of biosynthetic FeS_2 nanoparticles (at high concentrations) has enormous potential as an effective new generation antimicrobial agent to fight both Gram-positive and Gram-negative bacterial pathogens [30,31]. (see Fig. 9).

CONCLUSION

The present study achieved the environmentally benign synthesis of FeS_2 NPs using Artemisia herbal-alba as a bio friendly reducing and capping agent. Physic-chemical characterization of the synthesized NPs confirmed the formation of a pure pyrite crystalline phase with a crystalline size of 10 nm and quasi-spherical morphology with the plant phytochemicals contributing significantly towards stabilization of the nanoparticles for biocompatibility. The veridical activity of the NPs was found to exhibit a concentration-dependent inhibition of Staphylococcus aureus and Escherichia coli. Mediated by membrane damage and oxidative stress pathways, thus highlighting the significant potential of biosynthesized FeS_2 NPs as broad-spectrum antimicrobial agents for future biomedical and environmental applications.

CONFLICT OF INTEREST

The authors declare that there is no conflict of interests regarding the publication of this manuscript.

REFERENCES

1. Rai M, Yadav A, Gade A. Silver nanoparticles as a new generation of antimicrobials. Biotechnol Adv. 2009;27(1):76-83.
2. Synthesis of Nanomaterials. Nanocomposite Materials: CRC Press; 2016. p. 49-92. http://dx.doi.org/10.1201/9781315372310-10
3. Hulkoti NI, Taranath TC. Biosynthesis of nanoparticles using microbes—A review. Colloids Surf B Biointerfaces. 2014;121:474-483.
4. Iravani S. Green synthesis of metal nanoparticles using plants. Green Chem. 2011;13(10):2638.
5. Ahmed S, Ahmad M, Swami BL, Ikram S. A review on plants extract mediated synthesis of silver nanoparticles for antimicrobial applications: A green expertise. Journal of Advanced Research. 2016;7(1):17-28.
6. Bhattacharjee S, Habib F, Darwish N, Shanableh A. Iron sulfide nanoparticles prepared using date seed extract: Green synthesis, characterization and potential application for removal of ciprofloxacin and chromium. Powder Technol. 2021;380:219-228.
7. Koul B, Taak P, Kumar A, Kumar A, Sanyal I. Genus Psoralea: A review of the traditional and modern uses, phytochemistry and pharmacology. J Ethnopharmacol. 2019;232:201-226.
8. Efferth T, Herrmann F, Tahrani A, Wink M. Cytotoxic activity of secondary metabolites derived from Artemisia annua L. towards cancer cells in comparison to its designated active constituent artemisinin. Phytomedicine. 2011;18(11):959-969.
9. Saif S, Tahir A, Chen Y. Green Synthesis of Iron Nanoparticles and Their Environmental Applications and Implications. Nanomaterials. 2016;6(11):209.
10. Mohammed AS, Fahad OA. Sensitivity enhancement for NO2 gas sensor based on Alq3:TiO_2. AIP Conference Proceedings: AIP Publishing; 2021. p. 040008.
11. Dyusebaeva M, Berillo D, Yesbussinova Z, Ibragimova N, Shepilov D, Sydykbayeva S, et al. Green Synthesis and Characterization of Silver Nanoparticles Using Artemisia terrae-albae Extracts and Evaluation of Their Cytogenotoxic Effects. Int J Mol Sci. 2025;26(15):7499.
12. Mohaisen MA, Sirhan MM. Study of Fe_3O_4-NPs Coated with an Alcoholic Extract of C. Spinosa to Identify Appropriate IC50 HTC116 Cancer Cells. Pakistan Journal of Analytical and Environmental Chemistry. 2024;25(1):99-112.
13. Alshammari AF, Ouni S, Bouzidi M, Alshammari AS, Alzahrani EA, Alismail H, et al. Green synthesis and enhanced photocatalytic activity of ZnSe nanoparticles capped with

Artemisia herba-alba and calligonum plants extracts. Sci Rep. 2026;16(1).
14. Begum SK, Shabnam D, Haque N, Alam MJ, Ferdous J, Nur UJB, et al. Green synthesis of magnetite (Fe3O4) and hematite (Fe_2O_3) nanoparticles using Moringa oleifera and Psidium guajava leaf extracts for sustainable applications. Sci Rep. 2025;15(1).
15. Fahad OA, Abdulkareem FA, Mohammed AS, Kareem OA. Produce of Selenium Nanoparticles by Pulsed Laser Ablation for Anticancer Treatments. International Journal of Nanoscience. 2021;20(06).
16. Hasan H, Arshad F, Sk MP. Mechanochemical conversion of elemental sulfur into functional sulfur nanomaterials for promising applications. RSC Mechanochemistry. 2025;2(6):786-801.
17. Balouiri M, Sadiki M, Ibnsouda SK. Methods for in vitro evaluating antimicrobial activity: A review. Journal of Pharmaceutical Analysis. 2016;6(2):71-79.
18. Patra JK, Baek K-H. Antibacterial Activity and Synergistic Antibacterial Potential of Biosynthesized Silver Nanoparticles against Foodborne Pathogenic Bacteria along with its Anticandidal and Antioxidant Effects. Front Microbiol. 2017;08.
19. Editorial Board. J Microbiol Methods. 2022;200:106570.
20. Alatawi OM, Salim Albalawi AMA, Al Marji MA, Alyan MS, Al Anzi NM, Alamrani NS, et al. Identifying the Active Chemical Ingredients in Extracts of Certain Plants with Medicinal Properties used for the Treatment of Intestinal Diseases. Oriental Journal Of Chemistry. 2026;1(42):343.
21. Purnama H, Hanifa FK, Paldefi CR. Eco-Friendly Biosynthesis of Iron Oxide Nanoparticles Using Psidium guajava Leaf Extract for Photocatalytic Degradation of Methylene Blue. MEST 2025; 2026/05/25: MDPI; 2026. p. 13.
22. Shanmugam R, Tharani M, Abullais SS, Patil SR, Karobari MI. Black seed assisted synthesis, characterization, free radical scavenging, antimicrobial and anti-inflammatory activity of iron oxide nanoparticles. BMC Complementary Medicine and Therapies. 2024;24(1).
23. Esmaeili H, Asghartabar Kashi F, Moradi Alvand Z, Parseghian L, Askari F, Rafati H. Green synthesized iron oxide (Fe_2O_3) nanoparticle affects the germination and growth-related characteristics of different basil (Ocimum basilicum L.) cultivars. Sci Rep. 2025;15(1).
24. Yuan Y, Wang L, Gao L. Nano-Sized Iron Sulfide: Structure, Synthesis, Properties, and Biomedical Applications. Frontiers in Chemistry. 2020;8.
25. Hamid NM, Abed HA, Fahad OA. Evaluation of Antibacterial Effects of Silver Nanoparticles Synthesized via Pulsed Laser Ablation at Different Laser Energies. Lasers in Manufacturing and Materials Processing. 2025;12(3):488-497.
26. Mirali S, Heidari M, Ahmadi M, Rezaee A. Green synthesis of pyrite nanoparticles: nanozyme activity and kinetic studies. Chemical Papers. 2025;79(4):2375-2387.
27. Synthesis and Characterization of Fe_3O_4-NPs from Leaves C. Spinosa Extracts and their Anti-Microbial Activity. Nanotechnology Perceptions. 2024;20(3).
28. He S, Chen J, Zhao J, Wang Z, Wu R, Zhang Y. Highly efficient sterilization of biogenic FeS2 nanoparticles: Mechanism and inhibition of antibiotic resistance. Chem Eng J. 2025;509:160975.
29. Supplemental Information 2: Agar well diffusion assay. PeerJ.
30. Chung E, Ren G, Johnston I, Matharu RK, Ciric L, Walecka A, et al. Applied Methods to Assess the Antimicrobial Activity of Metallic-Based Nanoparticles. Bioengineering. 2023;10(11):1259.
31. Hanfoosh SM, Aadim KA, Razeg KH. Using the Plasma Jet Method to Create Zinc Nanoparticles and Study Their Structural and Optical Properties as an NH_3 Gas Sensor. International Journal of Nanoscience. 2024;23(06).